Journal of Alloys and Compounds 509 (2011) 5596–5599

Contents lists available at ScienceDirect

Journal of Alloys and Compounds

journal homepage: www.elsevier.com/locate/jallcom

Photoluminescent properties of $LiSr_xBa_{1-x}PO_4:RE^{3+}$ (RE = Sm^{3+}, Eu^{3+}) f–f transition phosphors

Dong Tu, Yujun Liang*, Rong Liu, Zheng Cheng, Fan Yang, Wenlong Yang

Faculty of Materials Science and Chemical Engineering, China University of Geosciences, Wuhan 430074, China

ARTICLE INFO

Article history:
Received 24 August 2010
Received in revised form 14 February 2011
Accepted 16 February 2011
Available online 23 February 2011

Keywords:
f–f transition
Phosphor
Sm^{3+}
Eu^{3+}

ABSTRACT

Rare-earth ions (Sm^{3+} or Eu^{3+}) doped $LiSr_xBa_{1-x}PO_4$ (x = 0, 0.2, 0.4, 0.6, 0.8, 1.0) f–f transition phosphor powders were prepared by a high temperature solid-state reaction. The resulted phosphors were characterized by X-ray diffraction (XRD) and photoluminescence (PL) spectroscopy. The results of XRD indicate that the phase structure of the sample changes from $LiBaPO_4$ to $LiSrPO_4$ when x changes from 0 to 1.0. The excitation spectra indicate that only direct excitation of rare earth ions (Sm^{3+} or Eu^{3+}) can be observed. The doped rare earth ions show their characteristic emission in $LiSr_xBa_{1-x}PO_4$, i.e., Eu^{3+} $^5D_0$–^7F_J (J = 0, 1, 2, 3, 4), Sm^{3+} $^4G_{5/2} \rightarrow {}^6H_J$ (J = 5/2, 7/2, 9/2, 11/2), respectively. The dependence of the emission intensities of the $LiSr_xBa_{1-x}PO_4:Sm^{3+}$ and $LiSr_xBa_{1-x}PO_4:Eu^{3+}$ phosphors on the x value and Ln^{3+} (Ln^{3+} = Sm^{3+}, Eu^{3+}) concentration is also investigated.

1. Introduction

Rare earth ions activated phosphors have attracted much attention of scientists due to their unique electronic, optical and chemical properties resulted from the 4f shell of the ion; also the progress in the development of the phosphors is directly related to the understanding of the physical processes of energy absorption and relaxation [1–3]. Thus, the f–f transition absorption and emission of the trivalent lanthanide ions in crystalline hosts is receiving more attention due to the applications as optical materials emitting in the visible and near-IR regions [4,5].

Phosphate compounds are known as multifunctional materials. In particular, orthophosphate have been extensively investigated due to their structural diversity. This makes them suitable as hosts to accommodate active rare earth ions. The luminescence of RE-doped phosphates usually has a high thermal stability [6], also rare earth doped luminescent materials have considerable practical applications in devices involving the artificial production of light, such as cathode ray tubes, lamps, X-ray detectors and LEDs, etc. [7–11]. As an activator of red luminescent materials, Eu^{3+} ion is widely used in color television and lamp phosphors [12–14]. The Sm^{3+} ion is also very important lanthanide ion for optical and other applications. For example $KBaPO_4:Sm^{3+}$ can be used for white light-emitting diodes [15].

Recently, orthophosphates with general formula $ABPO_4$ (A and B are mono- and divalent cations, respectively) have attracted great attention. For example, $LiSrPO_4$, $LiCaPO_4$, $NaCaPO_4$ and $KSrPO_4$ have been found to be the new luminescence hosts. In 2010, Yan Chen et al. reported an intense green emitting $LiSrPO_4:Eu^{2+}$, Tb^{3+} for phosphor-converted LED [16]. According to the new reports, More et al. [17] have studied the luminescence of $LiCaPO_4:Eu^{2+}$ phosphor. Shinde et al. [18] have investigated the photoluminescence properties of Dy^{3+}, Mn^{2+} or Gd^{3+} doped $NaCaPO_4$ phosphors, which have served as efficient phosphors in many industrial applications. Additionally, Zhang et al. [19] have also reported that $KSrPO_4:Tb^{3+}$ phosphor under vacuum ultraviolet excitation. However, to the best of our knowledge, there is no study devoted to the photoluminescence properties of $LiSr_xBa_{1-x}PO_4:RE^{3+}$ (RE = Sm^{3+}, Eu^{3+}) phosphors.

In this study, the f–f transition phosphors $LiSr_xBa_{1-x}PO_4:RE^{3+}$ (RE = Sm^{3+}, Eu^{3+}) have been prepared and characterized. The emission intensity of the phosphors has been successfully adjusted by controlling the phase structure of phosphor samples. The effects of Sm^{3+} and Eu^{3+} content on the luminescence properties of the phosphors have also been discussed.

2. Experimental

The $LiSr_xBa_{1-x}PO_4:RE^{3+}$ (RE = Sm^{3+}, Eu^{3+}) phosphors were synthesized through the solid-state reaction technique. Stoichiometric amounts of $SrCO_3$ (AR), $BaCO_3$ (AR), Li_2CO_3 (AR), $NH_4H_2PO_4$ (AR), Sm_2O_3 (99.99%) and Eu_2O_3 (99.99%) were mixed and grounded thoroughly, and then the resulting mixture was sintered at 1200 °C for 5 h in the air.

The crystal structures of products were recorded with Japan D/Max-3B X-ray diffraction (XRD) with Cu Kα (λ = 1.5418 Å) radiation generated at 30 kV/30 Ma, the powder diffraction patterns were collected within the 2θ range 10–70°, at the stepped scan rate of 0.001° per step and the count time of 0.05 s per step. The excitation and emission spectra were taken on a FluoroMax-4p spectrofluorometer

* Corresponding author. Tel.: +86 27 67884814; fax: +86 27 67883733.
E-mail address: yujunliang@sohu.com (Y. Liang).

0925-8388/$ – see front matter © 2011 Published by Elsevier B.V.
doi:10.1016/j.jallcom.2011.02.077

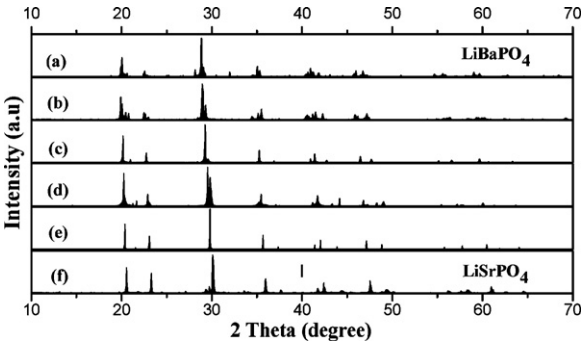

Fig. 1. X-ray powder diffraction patterns of phosphor samples $LiSr_xBa_{1-x}PO_4:Sm^{3+}$ ($x = 0, 0.2, 0.4, 0.6, 0.8, 1.0$): (a) $x = 0$, (b) $x = 0.2$, (c) $x = 0.4$, (d) $x = 0.6$, (e) $x = 0.8$ and (f) $x = 1.0$.

Table 1
The shift of the strongest diffraction peak of $LiBaPO_4$ to higher diffraction angle with the increase of x in phosphor samples $LiSr_xBa_{1-x}PO_4:Sm^{3+}$.

Samples	$X = 0$	$X = 0.2$	$X = 0.4$	$X = 0.6$	$X = 0.8$	$X = 1.0$
2θ value	28.846	28.946	29.255	29.535	29.815	30.115

equipped with a 150 W xenon lamp as the excitation source. All the measurements were performed at room temperature.

3. Results and discussion

Fig. 1 shows the XRD patterns of $LiSr_xBa_{1-x}PO_4:Sm^{3+}$ ($x = 0$, 0.2, 0.4, 0.6, 0.8, 1.0) phosphor samples and JCPDS Card 14-0270 for $LiBaPO_4$ (a) and 14-0202 for $LiSrPO_4$ (f) as references. With the addition of Sr, some new peaks appear due to the orthorhombic phase of $LiSrPO_4$ (Fig. 1(b)–(e)), indicating $LiSrPO_4$ phase is formed. With the increase of the value of x, the diffraction peaks of $LiSrPO_4$ phase become sharper and stronger, whereas the diffraction peaks of $LiBaPO_4$ phase become weaker. Note that the diffraction peaks shift to higher angles with the increase of the Sr content, indicating that the size of the crystalline grains in the $LiSrPO_4$ phase is smaller than that in the $LiBaPO_4$ phase. As we all know, the ionic radius of Sr^{2+} (0.126 nm) is smaller than that of Ba^{2+} (0.142 nm), the replacement of Ba^{2+} by Sr^{2+} should decrease the lattice parameter of $LiBaPO_4$. Table 1 summaries the strongest diffraction peak of the $LiSr_xBa_{1-x}PO_4$. The 2θ values of these peaks change from 28.846° to 30.115° when x change from 0 to 1.0.

Photoluminescence excitation and emission spectra of $LiSr_{0.8}Ba_{0.2}PO_4:Sm^{3+}$ powder phosphors are shown in Fig. 2. The excitation spectrum of Sm^{3+}-doped $LiSr_{0.8}Ba_{0.2}PO_4$ (Fig. 2(a)) monitored at 595 nm consists of several bands centered at 360, 373, 401 and 467 nm, which is the characteristic f–f transitions of Sm^{3+} ions. The strongest peak at 401 nm is attributed to the $^6H_{5/2} \rightarrow {}^4G_{7/2}$ transition of Sm^{3+}. There is no obvious charge-transfer absorption of Sm^{3+}–O^{2-} interaction or host absorption band as usual. This is because Sm^{3+} ions interaction with the host lattice is very weak, and no energy transfer occurs between Sm^{3+} and host [11]. Upon the excitation at 401 nm, the emission spectrum of Sm^{3+}-doped phosphor consists of the characteristic emission lines of Sm^{3+}, i.e., 559 nm ($^4G_{5/2} \rightarrow {}^6H_{5/2}$), 595 nm ($^4G_{5/2} \rightarrow {}^6H_{7/2}$), 641 nm ($^4G_{5/2} \rightarrow {}^6H_{9/2}$) and 707 nm ($^4G_{5/2} \rightarrow {}^6H_{11/2}$) with the strongest peak at 595 nm (Fig. 2(b)). The effect of doped concentration of Sm^{3+} on the luminescent intensity is also investigated. Five different amounts, 1, 3, 5, 7, 9 mol% of Sm^{3+} are introduced into $LiSr_{0.8}Ba_{0.2}PO_4$. The emission spectra of phosphors with different Sm^{3+} concentrations (shown in Fig. 3) indicate that the luminescent intensity increases with the increment of doping concentration, and reaches the maximum at the doping concentration of 5 mol%. At 7 mol%, the luminescence

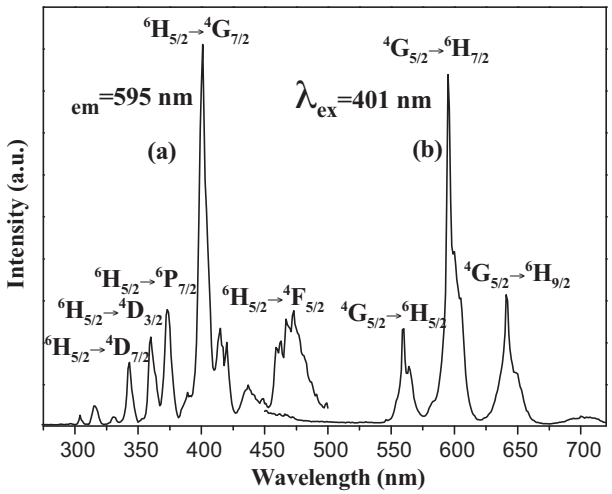

Fig. 2. Photoluminescence emission and excitation spectra of $LiSr_{0.8}Ba_{0.2}PO_4:Sm^{3+}$ powder phosphor.

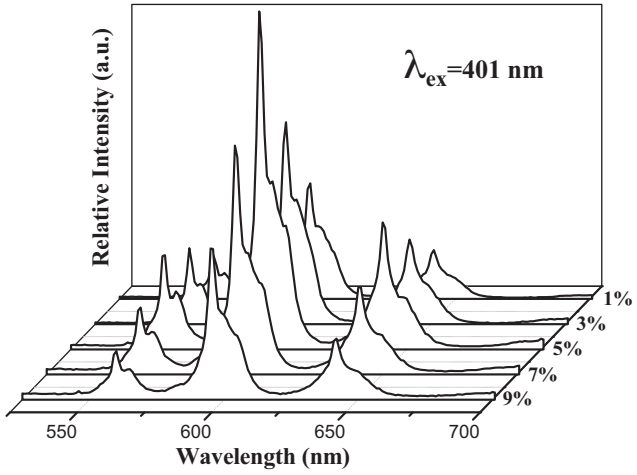

Fig. 3. Photoluminescence emission spectra of $LiSr_{0.8}Ba_{0.2}PO_4:Sm^{3+}$ with different Sm^{3+} concentration.

intensity decreases, which indicates concentration quenching effect occurs when the concentration of lanthanide ion is higher than 5 mol%.

Fig. 4 shows the photoluminescence excitation and emission spectra of $LiSr_{0.8}Ba_{0.2}PO_4:Eu^{3+}$ powder phosphor. The excitation spectrum of $LiSr_{0.8}Ba_{0.2}PO_4:Eu^{3+}$ phosphor by monitoring the emission at 614 nm (Fig. 4(a)) consists of a weak broad band from 200 to 300 nm, which is caused by the oxygen-to-europium charge-transfer (C-T) transition, and sharp lines in the 350–500 nm range peaking at 361 nm ($^7F_0$–$^5D_4$), 381 nm ($^7F_0$–^5G_J), 393 nm ($^7F_0$–$^5L_6$) and 464 nm ($^7F_0$–$^5D_2$) caused by the f–f transitions between the ground level $^7F_0$ and the excited levels $^5D_4$, ^5G_J, $^5L_6$, $^5D_2$ of Eu^{3+} ions. The emission spectrum (Fig. 4(b)) consists of a series of typical linear emission peaks of Eu^{3+} ascribed to the transition of $^5D_0 \rightarrow {}^7F_0$ (577 nm), $^5D_0 \rightarrow {}^7F_1$ (587 nm), $^5D_0 \rightarrow {}^7F_2$ (614 nm), $^5D_0 \rightarrow {}^7F_3$ (651 nm) and $^5D_0 \rightarrow {}^7F_4$ (695 nm). $^5D_0 \rightarrow {}^7F_1$ lines originate from the magnetic dipole transition and the $^5D_0 \rightarrow {}^7F_2$ lines arise from the electric dipole transition and its intensity is very sensitive to the site symmetry of the Eu^{3+} ions. The Eu^{3+} ions generally occupy the substitution sites of Sr^{2+} ions in $LiSr_xBa_{1-x}PO_4:Eu^{3+}$ phosphors, making the $^5D_0 \rightarrow {}^7F_1$ and $^5D_0 \rightarrow {}^7F_2$ transitions allowed. In this situation, the $^5D_0 \rightarrow {}^7F_0$ transition is in principle forbidden due to the same total angular momentum. Thus, the corresponding peak

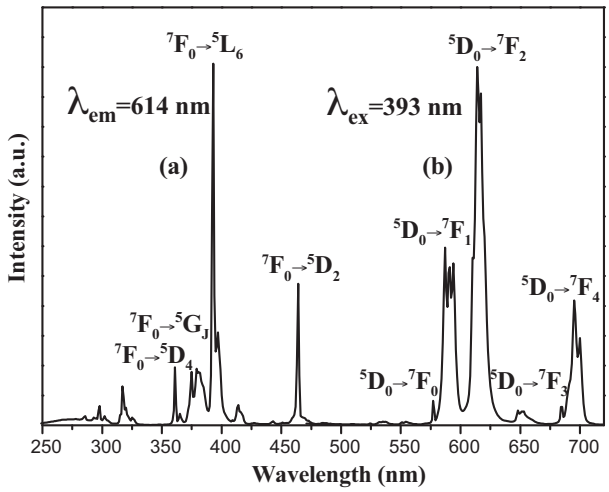

Fig. 4. Photoluminescence emission and excitation spectra of $LiSr_{0.8}Ba_{0.2}PO_4:Eu^{3+}$ powder phosphor.

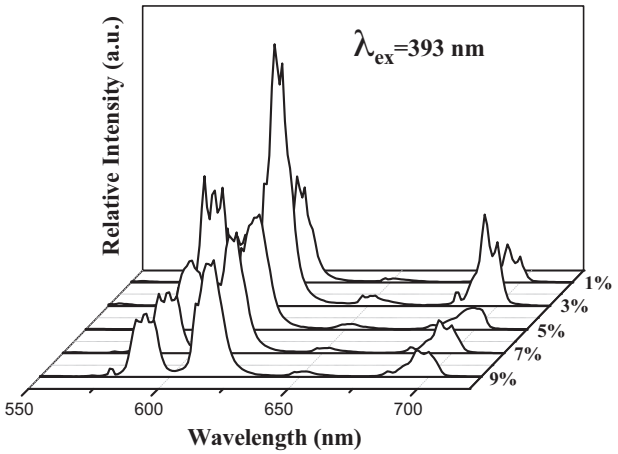

Fig. 5. Photoluminescence emission spectra of $LiSr_{0.8}Ba_{0.2}PO_4:Eu^{3+}$ with different Eu^{3+} concentration.

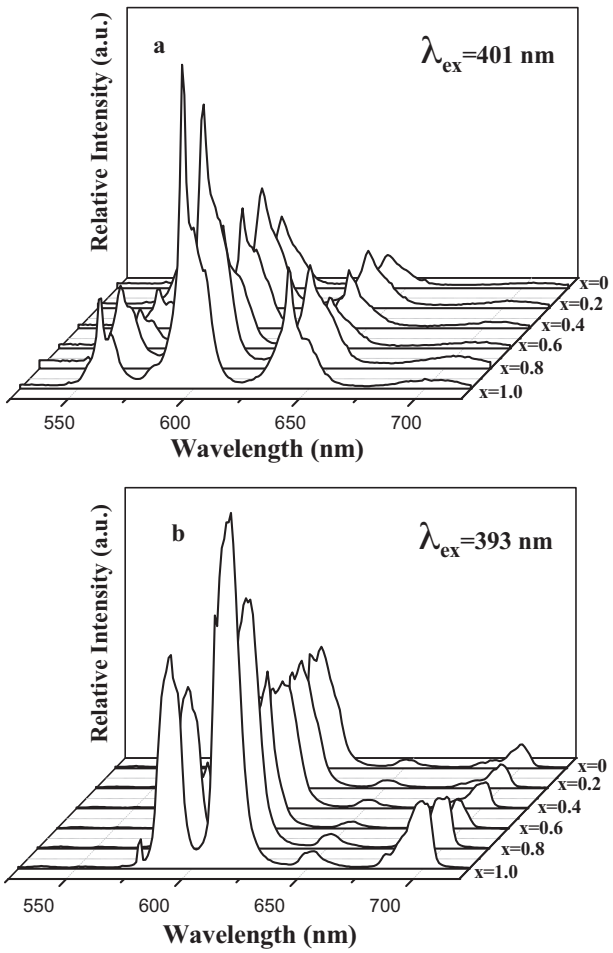

Fig. 6. Photoluminescence emission spectra of phosphor samples: (a) $LiSr_xBa_{1-x}PO_4:Sm^{3+}$ (5%) and (b) $LiSr_xBa_{1-x}PO_4:Eu^{3+}$ (5%) (x = 0, 0.2, 0.4, 0.6, 0.8, 1.0).

should be inexistent or very weak in the PL emission spectrum [20–22]. The emission spectra of phosphors $LiSr_xBa_{1-x}PO_4:Eu^{3+}$ with different Eu^{3+} concentrations are illustrated in Fig. 5. The emission intensity of Eu^{3+} first increases with increasing doping concentration, reaching a maximum at 3 mol%, and then decreases with further increasing Eu^{3+} concentration due to concentration quenching. Thus the optimum concentration for Eu^{3+} red emission is 3 mol%.

The substitution of Sr into Ba site also leads to the remarkable enhancement of the fluorescent emission intensity of the $LiBaPO_4:Sm^{3+}$ (5%) and $LiBaPO_4:Eu^{3+}$ (5%) phosphors, as shown in Fig. 6, the emission intensity increases with increasing the value of x. When x equal to 1.0, the luminescence intensity reaches maximum, 4.5 times higher than that of the Sr-free materials for $LiSr_xBa_{1-x}PO_4:Sm^{3+}$ and 2.7 times for $LiSr_xBa_{1-x}PO_4:Eu^{3+}$. The $ABPO_4$ (A: alkaline metals, B: alkaline earth metals) phosphates with A cations and B in tetrahedral environment belong to a wide structural family in which the BPO_4^- tetrahedra framework shows four-, six- and eight-membered rings, like some silica or silicate forms. The tunnels perpendicular to the six-membered rings form irregular open cavities that host the monovalent cation [23]. Depending on the small ionic radius of Li^+ (0.059 nm), the orthorhombic phase of $LiBaPO_4$ is observed in Fig. 1(a). At the same time, it should be realized that $LiBaPO_4$ structure contains two inequivalent barium sites [24]. It is often assumed that in such systems substitution into both sites occurs randomly. However, if we assume that due to the large difference in ionic sizes of Ba^{2+} (0.142 nm) and Sr^{2+} (0.126 nm), strontium ions would enter preferentially into one site, and the whole structure would accommodate the distortion. As a consequence, Sm^{3+} and Eu^{3+} would prefer to Sr site due to the similarity of ionic radius (Sm^{3+} ionic radius 0.104 nm, Eu^{3+} ionic radius 0.109 nm) [25]. Thus, the fluorescence intensity shown by the synthesized materials should enhance with the increase of Sr fraction in Ba sites. In addition, the least radius (0.059 nm) of Li^+ ion is helpful for Sm^{3+} and Eu^{3+} ions entering the host material [26]. The emission peak shifts a little, from 614 to 616 nm with the x value in $LiSr_xBa_{1-x}PO_4:Eu^{3+}$ increases, which may be ascribed to the increase of the crystal field strength.

Fig. 7 shows the Commission International de l'Eclairage (CIE) chromaticity coordinates at 293 K for $LiSr_xBa_{1-x}PO_4:Sm^{3+}$ (x = 0, 0.2, 0.8, 1.0) and $LiSr_xBa_{1-x}PO_4:Eu^{3+}$ (x = 0, 0.2, 0.8, 1.0). The (x, y) coordinates vary systematically from (0.453, 0.368), (0.486, 0.371), (0.510, 0.389) to (0.540, 0.397), corresponding to hues of white, white, orange, orange for $LiSr_xBa_{1-x}PO_4:Sm^{3+}$ (x = 0, 0.2, 0.8, 1.0); while for $LiSr_xBa_{1-x}PO_4:Eu^{3+}$ (x = 0, 0.2, 0.8, 1.0), the (x, y) coordinates vary from (0.603, 0.361), (0.609, 0.360), (0.623, 0.362) to (0.628, 0.362), all corresponding to hues of reddish orange. The above results indicate that $LiSr_xBa_{1-x}PO_4:Sm^{3+}$ and $LiSr_xBa_{1-x}PO_4:Eu^{3+}$ may be good candidates for the application of white LEDs.

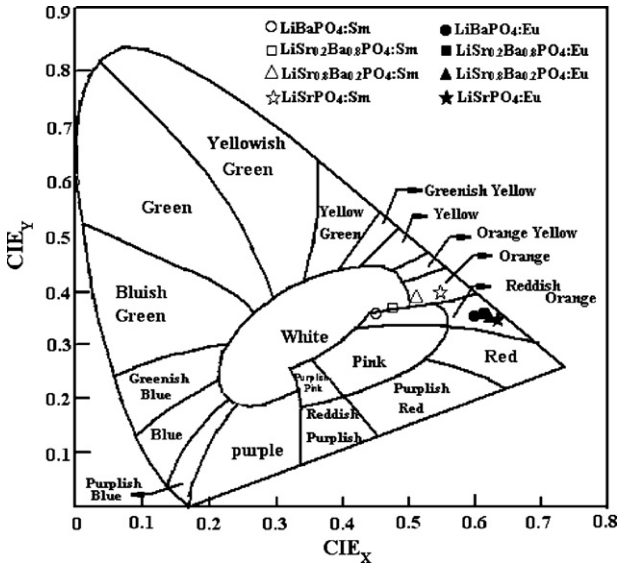

Fig. 7. The Commission International de l'Eclairage (CIE) chromaticity coordinates for $LiSr_xBa_{1-x}PO_4:Sm^{3+}$ (5%) and $LiSr_xBa_{1-x}PO_4:Eu^{3+}$ (5%) (x = 0, 0.2, 0.8, 1.0).

4. Conclusions

$LiSr_xBa_{1-x}PO_4:Sm^{3+}$ and $LiSr_xBa_{1-x}PO_4:Eu^{3+}$ f–f transition phosphors were successfully prepared by the high temperature solid state reaction. The XRD data suggested the host phase changed from $LiBaPO_4$ to $LiSrPO_4$ phase when the value of x changed from 0 to 1.0. The substitution of Sr^{2+} ions for Ba^{2+} ions occurred in $LiBaPO_4$ structure. The doped rare earth ions (Sm^{3+} and Eu^{3+}) showed their characteristic emission in $LiSr_xBa_{1-x}PO_4$. The emission intensity can be tuned by the doping concentration of Ln^{3+} ions and the value of x. The optimum concentrations for Sm^{3+} and Eu^{3+} were determined to be 5 and 3 mol% in $LiSr_xBa_{1-x}PO_4$, respectively. All the results indicated that $LiSr_xBa_{1-x}PO_4:Sm^{3+}$ and $LiSr_xBa_{1-x}PO_4:Eu^{3+}$ phosphors had potential application in the LED field.

Acknowledgements

The authors acknowledge the Fundamental Research Funds for the Central Universities (no. CUG090108) and Guangdong Province Enterprise-University-Academy Collaborative Project (no. 2010B090400437) for financial support.

References

[1] M. Guzik, T. Aitsalo, W. Szuszkiewicz, J. Holsa, B. Keller, J. Legendziewicz, J. Alloys Compd. 380 (2004) 368–375.
[2] L. Schwarz, B. Finke, M. Kloss, A. Rohmann, U. Sasum, D. Haberland, J. Lumin. 72–74 (1997) 257–259.
[3] J. Legendziewicz, M. Guzik, J. Cybinska, Opt. Mater. 31 (2009) 567–574.
[4] J. Wang, X. Jing, C. Yan, J. Lin, F. Liao, J. Lumin. 121 (2006) 57–61.
[5] S. Neeraj, N. Kijima, A.K. Cheetham, Chem. Phys. Lett. 387 (2004) 2–6.
[6] I.M. Nagpure, K.N. Shinde, V. Kumar, O.M. Ntwaeaborwa, S.J. Dhoble, H.C. Swart, J. Alloys Compd. 492 (2010) 384–388.
[7] X. Su, B. Yan, J. Alloys Compd. 421 (2006) 273–278.
[8] L. Hesselink, S.S. Orlov, A. Liu, A. Akella, D. Lande, R.R. Neurgaonkar, Science 282 (1998) 1089–1094.
[9] D.M. Burland, R.D. Miller, C.A. Walsh, Chem. Rev. 94 (1994) 31–75.
[10] L.L. Beecroft, C.K. Ober, Chem. Mater. 9 (1997) 1302–1317.
[11] Y.-C. Li, Y.-H. Chang, Y.-Feng Lin, Y.-S. Chang, Y.-J. Lin, J. Alloys Compd. 439 (2007) 367–375.
[12] B. Yan, J. Gu, J. Alloys Compd. 479 (2009) 536–540.
[13] H. Song, B. Chen, B. Sun, J. Zhang, S. Lu, Chem. Phys. Lett. 372 (2003) 368–372.
[14] G. Blasse, B.C. Grabmaier (Eds.), Luminsecent Materials, Springer, Berlin, 1994.
[15] C.C. Lin, Y.S. Tang, S.F. Hu, R.S. Liu, J. Lumin. 129 (2009) 1682–1684.
[16] Y. Chen, J. Wang, X. Zhang, G. Zhang, M. Gong, Q. Su, Sens. Actuators, B 148 (2010) 259–263.
[17] S.D. More, S.P. Wankhede, M. Kumar, G.S.V. Chourasiya, S.V. Moharil, Radiat. Meas. 46 (2011) 196–198.
[18] K.N. Shinde, S.J. Dhoble, A. Kumar, Physica B 406 (2011) 94–99.
[19] F. Zhang, Y. Wang, J. Liu, J. Alloys Compd. 509 (2011) 3852–3854.
[20] P. Chen, X. Ma, D. Yang, J. Alloys Compd. 431 (2007) 317–320.
[21] A. Pierrard, P. Gredin, N. Dupont, A. de Kozak, B. Piriou, J. Alloys Compd. 289 (1999) 71–80.
[22] M. Guzik, E. Tomaszewicz, S.M. Kaczmarek, J. Cybinska, H. Fuks, J. Non-Cryst. Solids 356 (2010) 1902–1907.
[23] R.A Benhamou, G. Wallez, P. Loiseau, B. Viana, M. Elaatman, M. Daoud, A. Zegzouti, J. Solid State Chem. 183 (2010) 2082–2086.
[24] Z.C. Wu, J. Liu, M.L. Gong, Q. Su, J. Electrochem. Soc. 156 (2009) H153–H156.
[25] C.-W. Lee, V. Petrykin, M. Kakihana, J. Cryst. Growth 311 (2009) 647–650.
[26] X. Li, L. Guan, X. Li, J. Wen, Z. Yang, Powder Technol. 200 (2010) 12–15.